Hindawi Publishing Corporation
Mathematical Problems in Engineering
Volume 2011, Article ID 534968, 23 pages
doi:10.1155/2011/534968

Research Article

Dynamic Analysis of Partially Embedded Structures Considering Soil-Structure Interaction in Time Domain

Sanaz Mahmoudpour, Reza Attarnejad, and Cambyse Behnia

School of Civil Engineering, University of Tehran, Tehran, Iran

Correspondence should be addressed to Reza Attarnejad, attarnjd@ut.ac.ir

Received 7 June 2011; Revised 8 August 2011; Accepted 12 August 2011

Academic Editor: Delfim Soares Jr.

Analysis and design of structures subjected to arbitrary dynamic loadings especially earthquakes have been studied during past decades. In practice, the effects of soil-structure interaction on the dynamic response of structures are usually neglected. In this study, the effect of soil-structure interaction on the dynamic response of structures has been examined. The substructure method using dynamic stiffness of soil is used to analyze soil-structure system. A coupled model based on finite element method and scaled boundary finite element method is applied. Finite element method is used to analyze the structure, and scaled boundary finite element method is applied in the analysis of unbounded soil region. Due to analytical solution in the radial direction, the radiation condition is satisfied exactly. The material behavior of soil and structure is assumed to be linear. The soil region is considered as a homogeneous half-space. The analysis is performed in time domain. A computer program is prepared to analyze the soil-structure system. Comparing the results with those in literature shows the exactness and competency of the proposed method.

1. Introduction

In a dynamic soil-structure interaction problem, the structure is supported by an unbounded soil medium subjected to a dynamic load like an earthquake. The dynamic response of the structure is affected by the interaction between the structure, foundation, and soil.

In dynamic soil-structure interaction analysis, usually the higher modes of the structure are affected significantly by soil-structure interaction (SSI) effects. As the influence of higher modes on the seismic response of flexible high structures with small mass remains small, the SSI effects are negligible for these structures. On the other hand for stiff and massive structures on relatively soft ground, the effects of SSI are noticeable and lead to an increase in the natural period and a change in the damping ratio of the system [1–3]. Effects of

interaction can be expressed as inertial interaction and kinematic interaction. The interaction effect associated with the stiffness of the structure is termed kinematic interaction, and the corresponding mass-related effect is called inertial interaction [4]. Jennings and Bielak [5], Veletsos and Nair [6], and Bielak [7] studied effects of inertial interaction, and Todorovska and Trifunac [8], Aviles and Perez-Rocha [9], Betti et al. [10], and Aviles et al. [11] studied the effects of kinematic interaction.

In dynamic soil-structure interaction problems, analysis methods can be classified into three groups [12]: (1) time domain and frequency domain analysis methods, (2) substructure method and direct method, (3) rigorous methods and approximate simple physical models.

Time domain methods are capable of studying nonlinear behavior of soil medium, effects of pore water, and nonlinear conditions along the interface between soil and structure. In frequency domain, the solving procedure is easier than time domain but it can deal only with linear aspects.

In substructure, method the whole media is represented by an impedance matrix which could be attached to the dynamic stiffness of the structure. This hypothesis renders the soil-structure interaction problem simpler and reduces the analysis efforts. In direct method the soil region near the structure is modeled directly; hence, complex geometry, variations of soil properties, and nonlinear behavior of the medium could be considered. As mentioned in this method, the unbounded soil medium is replaced by a bounded region with artificial boundaries. It should be considered that in the numerical modeling of unbounded media, the boundaries should be expressed, so that the radiation condition is satisfied exactly, and the wave energy dissipates in the medium. Several studies have been performed, and methods to impose a wave-absorbing boundary condition have been proposed [13–17].

Simple physical models can be applied to help the analyst identify the key parameters of the dynamic system for preliminary design or investigate alternative designs. They are used to check the results of more rigorous procedures determined with sophisticated computer programs [12].

To solve the soil-structure interaction problems, several analytical and numerical methods have been developed. Applying analytical methods is limited to simple structures and uniform soil media, while numerical methods such as finite element method (FEM), infinite element method, and boundary element method (BEM) are widely used. The FEM method is well suited for nonhomogeneous, anisotropic materials of arbitrary-shaped structure with non-linear behavior [18]. BE methods require a fundamental solution satisfying the governing differential equations exactly [19–22]. This analytical solution is often complicated, exhibiting singularities. Certain shortage in modeling nonhomogeneous soil media is exhibited using BE methods. Cone models have been used to determine dynamic stiffness of foundations and the seismic effective foundation input motion as an alternative to rigorous boundary-element solutions [23–30]. The concept of infinite element method was introduced by Ungless [31] and Bettess [32, 33]. The concepts and formulation procedure in this method are similar to those of FEM methods. The scaled boundary finite element method (SBFEM) which is a semianalytical computational procedure can be used for modeling bounded and unbounded medium considering nonhomogeneous and incompressible material properties. This method has been applied to soil-structure interaction problems both in time and frequency domain by Wolf and Song [34, 35].

Combined models are used in soil-structure interaction analysis. The most widely used combined model is the coupled finite element and boundary element method in both time and frequency domain [36–38]. Qian et al. [39] Estorff and Prabucki [40], and Israil and Banerjee [41] used the coupled FEM-BEM model for analysis of homogeneous media.

Zhang et al. presented the analysis in time domain for layered soils [42]. Tanikulu et al. extended BEM formulation for infinite nonhomogeneous media [43]. They could model only three different layers. Coupled finite element-Infinite element models have been used in dynamic soil-structure interaction analysis [44–46]. Coupled finite element/boundary element/scaled boundary finite element model [47] has been used to solve soil-structure interaction problems.

Jeremić et al. [48] have studied the effects of nonuniformity of soils in large structures where they developed various models to simulate wave propagation through soils with elastoplastic behavior.

Ghannad and Mahsuli [49] studied the effect of foundation embedment using a simplified single degree of freedom model with idealized bilinear behavior for the structure and considered the soil as a homogeneous half-space as a discrete model based on cone model concepts. The foundation is modeled as a rigid cylinder embedded in the soil.

The scaled boundary finite element method is a boundary-element method based on finite elements. This method combines the advantages of the boundary and finite element methods. It also combines the advantages of the numerical and analytical procedures. This method can be applied in both frequency and time domains [35]. This method is a semianalytical procedure which transforms the partial differential equation to an ordinary differential equation using a virtual work statement as in finite elements. In this method, no fundamental solution is required, and no singular integrals occur. Only the boundary is discretized which results in a reduction of the spatial discretization by one. The analytical solution in the radial direction permits the boundary condition at infinity to be satisfied exactly [35]. A computer program named SIMILAR based on SBFEM is presented by Wolf and Song [50]. This program calculates the dynamic stiffness of the unbounded media in frequency and time domain.

In this study, the dynamic behavior of partially embedded structures is examined. The substructure method is used, and a coupled finite element, scaled boundary finite element model is applied. The scaled boundary finite element method is used to calculate the dynamic stiffness of the soil, and the finite element method is applied to analyze the dynamic behavior of the structure. In continuation, firstly, the equation of motion of the soil structure system in total and relative displacements is introduced. The dynamic stiffness matrix of the soil is obtained using SBFEM in the second section. In the third section, an iterative procedure is presented to calculate dynamic load using dynamic stiffness matrix of the soil. Applying Newmark method, the equation of motion of the system is solved, and the displacements of the structure are obtained. It is worth noting that although the formulation in the paper is not innovative, this is the first time a complete model of structure is studied and the dynamic response of the structure is examined. Previous studies have used simplified soil model or simplified structural model and/or both. Therefore, the present results seem to be the first ones obtained based on a complete soil-structure model. Moreover, from a practical point of view, the present results could lead to an interesting conclusion in the important topic of "choosing base shear level" which is not clearly defined in practice codes

Numerical examples are presented, and the final section is devoted to concluding remarks.

2. Equation of Motion

The dynamic behavior of the structure could be described by its static stiffness matrix $[K]$ and the mass matrix $[M]$. The equation of motion of the structure in total displacements in time

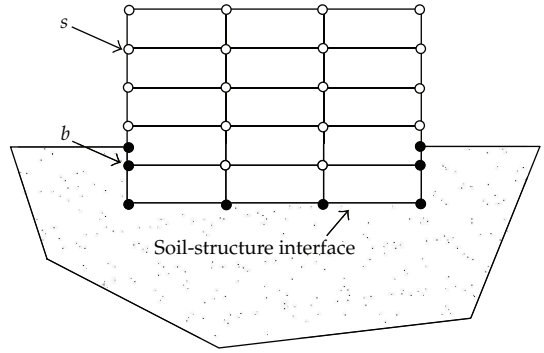

Figure 1: Soil-structure system.

domain is formulated as follows [35]:

$$\begin{bmatrix} [M_{ss}] & [M_{sb}] \\ [M_{bs}] & [M_{bb}] \end{bmatrix} \begin{Bmatrix} \{\ddot{u}_s^t(t)\} \\ \{\ddot{u}_b^t(t)\} \end{Bmatrix} + \begin{bmatrix} [K_{ss}] & [K_{sb}] \\ [K_{bs}] & [K_{bb}] \end{bmatrix} \begin{Bmatrix} \{u_s^t(t)\} \\ \{u_b^t(t)\} \end{Bmatrix} = \begin{Bmatrix} \{0\} \\ -\{R(t)\} \end{Bmatrix}. \tag{2.1}$$

Considering damping matrix of the structure, $[C]$, the above equation is written as follows:

$$\begin{bmatrix} [M_{ss}] & [M_{sb}] \\ [M_{bs}] & [M_{bb}] \end{bmatrix} \begin{Bmatrix} \{\ddot{u}_s^t(t)\} \\ \{\ddot{u}_b^t(t)\} \end{Bmatrix} + \begin{bmatrix} [C_{ss}] & [C_{sb}] \\ [C_{bs}] & [C_{bb}] \end{bmatrix} \begin{Bmatrix} \{\dot{u}_s^t(t)\} \\ \{\dot{u}_b^t(t)\} \end{Bmatrix} + \begin{bmatrix} [K_{ss}] & [K_{sb}] \\ [K_{bs}] & [K_{bb}] \end{bmatrix} \begin{Bmatrix} \{u_s^t(t)\} \\ \{u_b^t(t)\} \end{Bmatrix} = \begin{Bmatrix} \{0\} \\ -\{R(t)\} \end{Bmatrix}, \tag{2.2}$$

where $\{\ddot{u}^t\}$, $\{\dot{u}^t\}$, and $\{u^t\}$ are the acceleration, velocity, and displacement vectors of the structure. Subscripts are used to denote the nodes of the discretized system. As shown in Figure 1, nodes on the foundation structure interface are denoted by b, and the remaining nodes related to the structure are denoted by s. $\{R(t)\}$ denotes the interaction forces of the unbounded soil acting on the interface nodes of soil-structure system. The interaction forces of the soil depend upon the motion relative to the effective foundation input motion$\{u_b^g\}$. The interaction force-displacement relationship in the time domain is formulated as:

$$\{R(t)\} = \int_0^t [S^\infty(t-\tau)]\{u(\tau)\}d\tau, \tag{2.3}$$

where $[S^\infty(t)]$ is called the displacement unit impulse response matrix in time domain. The interaction force-displacement relationship can alternatively be written as

$$\{R(t)\} = \int_0^t [M^\infty(t-\tau)]\{\ddot{u}(\tau)\}d\tau, \tag{2.4}$$

in which $[M^\infty(t)]$ is the acceleration unit-impulse response matrix in time domain.

Superscript ∞ denotes the unbounded medium. For an unbounded medium initially at rest, we have

$$\begin{aligned} \{u(t=0)\} &= 0, \\ \{\dot{u}(t=0)\} &= 0. \end{aligned} \tag{2.5}$$

Substituting (2.6) in (2.1) results the equation of motion in total displacement [35]:

$$\begin{aligned} &\begin{bmatrix} [M_{ss}] & [M_{sb}] \\ [M_{bs}] & [M_{bb}] \end{bmatrix} \begin{Bmatrix} \{\ddot{u}_s^t(t)\} \\ \{\ddot{u}_b^t(t)\} \end{Bmatrix} + \begin{bmatrix} [C_{ss}] & [C_{sb}] \\ [C_{bs}] & [C_{bb}] \end{bmatrix} \begin{Bmatrix} \{\dot{u}_s^t(t)\} \\ \{\dot{u}_b^t(t)\} \end{Bmatrix} + \begin{bmatrix} [K_{ss}] & [K_{sb}] \\ [K_{bs}] & [K_{bb}] \end{bmatrix} \begin{Bmatrix} \{u_s^t(t)\} \\ \{u_b^t(t)\} \end{Bmatrix} \\ &\quad = \begin{Bmatrix} \{0\} \\ -\int_0^t [M^\infty(t-\tau)](\{\ddot{u}_b^t\} - \{\ddot{u}_g\})d\tau \end{Bmatrix}, \end{aligned} \tag{2.6}$$

in which $\{\ddot{u}_g\}$ is the ground motion acceleration induced to the base of the structure during an earthquake.

In this paper, the equation of motion of soil-structure system in relative displacement is used

$$\begin{aligned} &\begin{bmatrix} [M_{ss}] & [M_{sb}] \\ [M_{bs}] & [M_{bb}] \end{bmatrix} \begin{Bmatrix} \{\ddot{u}_s(t)\} \\ \{\ddot{u}_b(t)\} \end{Bmatrix} + \begin{bmatrix} [C_{ss}] & [C_{sb}] \\ [C_{bs}] & [C_{bb}] \end{bmatrix} \begin{Bmatrix} \{\dot{u}_s(t)\} \\ \{\dot{u}_b(t)\} \end{Bmatrix} + \begin{bmatrix} [K_{ss}] & [K_{sb}] \\ [K_{bs}] & [K_{bb}] \end{bmatrix} \begin{Bmatrix} \{u_s(t)\} \\ \{u_b(t)\} \end{Bmatrix} \\ &\quad = \begin{Bmatrix} -[M_{ss}]\{\ddot{u}_g\} \\ -[M_{sb}]\{\ddot{u}_g\} - \int_0^t [M^\infty(t-\tau)](\{\ddot{u}_b\})d\tau \end{Bmatrix}. \end{aligned} \tag{2.7}$$

As can be seen in (2.7), the unit impulse response matrix should be obtained a priori. The dynamic load on the right hand side of the equation is calculated a posteriori. In the next section, the unit impulse response matrix is obtained applying scaled boundary finite element method [35].

3. Obtaining Acceleration Unit-Impulse Response Matrix

The force displacement relationship in the frequency domain could be written as follows [35]:

$$\{R(\omega)\} = [M^\infty(\omega)](i\omega)^2\{u(\omega)\}, \tag{3.1}$$

where $\{R(\omega)\}$ and $\{u(\omega)\}$ are force and displacement in frequency domain. $[M^\infty(\omega)]$ is denoted as acceleration dynamic stiffness matrix in the frequency domain. The relationship between the acceleration and displacement dynamic stiffness matrices is

$$[M^\infty(\omega)] = \frac{[S^\infty(\omega)]}{(i\omega)^2}. \tag{3.2}$$

The scaled boundary finite element equation in dynamic stiffness for the unbounded medium is formulated as follows [35]:

$$\left([S^{\infty}(\omega)]+\left[E^{1}\right]\right)\left[E^{0}\right]^{-1}\left([S^{\infty}(\omega)]+\left[E^{1}\right]^{T}\right)-(s-2)[S^{\infty}(\omega)]-\omega[S^{\infty}(\omega)]_{,\omega}-\left[E^{2}\right]+\omega^{2}\left[M^{0}\right]=0, \tag{3.3}$$

in which $[E^0]$, $[E^1]$, and $[E^2]$ are coefficient matrices in the Scaled Boundary Finite Element method introduced in [35].

Dividing (3.3) by $(i\omega)^4$ and substituting (3.2) yields [35]

$$\begin{aligned}[M^{\infty}(\omega)]\left[E^{0}\right]^{-1}[M^{\infty}(\omega)]+\left[E^{1}\right]\left[E^{0}\right]^{-1}\frac{[M^{\infty}(\omega)]}{(i\omega)^{2}}+\frac{[M^{\infty}(\omega)]}{(i\omega)^{2}}\left[E^{0}\right]^{-1}\left[E^{1}\right]^{T}-s\frac{[M^{\infty}(\omega)]}{(i\omega)^{2}}\\ +\frac{1}{\omega}[M^{\infty}(\omega)]_{,\omega}-\frac{1}{(i\omega)^{4}}\left(\left[E^{2}\right]-\left[E^{1}\right]\left[E^{0}\right]^{-1}\left[E^{1}\right]^{T}\right)-\frac{1}{(i\omega)^{2}}\left[M^{0}\right]=0.\end{aligned} \tag{3.4}$$

Applying the inverse Fourier transformation to (3.4) results in

$$\begin{aligned}&\int_{0}^{t}[M^{\infty}(t-\tau)]\left[E^{0}\right]^{-1}[M^{\infty}(\tau)]d\tau+\left(\left[E^{1}\right]\left[E^{0}\right]^{-1}-\frac{s+1}{2}\right)\int_{0}^{t}\int_{0}^{\tau}[M^{\infty}(\tau')]\,d\tau'd\tau\\ &+\int_{0}^{t}\int_{0}^{\tau}[M^{\infty}(\tau')]d\tau'd\tau\left(\left[E^{0}\right]^{-1}\left[E^{1}\right]^{T}-\frac{s+1}{2}\right)\\ &+t\int_{0}^{t}[M^{\infty}(\tau)]d\tau-\frac{t^{3}}{6}\left(\left[E^{2}\right]-\left[E^{1}\right]\left[E^{0}\right]^{-1}\left[E^{1}\right]^{T}\right)H(t)-t\left[M^{0}\right]H(t)=0.\end{aligned} \tag{3.5}$$

The positive definite coefficient matrix $[E^0]$ is decomposed by Cholesky's method as follows:

$$\left[E^{0}\right]=[U]^{T}[U], \tag{3.6}$$

where $[U]$ is an upper-triangular matrix. Substituting (3.6) in (3.5) and premultiplying by $([U]^{-1})^{T}$ and postmultiplying by $[U]^{-1}$ yields

$$\begin{aligned}&\int_{0}^{t}[m^{\infty}(t-\tau)][m^{\infty}(\tau)]d\tau+\left[e^{1}\right]\int_{0}^{t}\int_{0}^{\tau}[m^{\infty}(\tau')]d\tau'd\tau+\int_{0}^{t}\int_{0}^{\tau}[m^{\infty}(\tau')]d\tau'd\tau\left[e^{1}\right]^{T}\\ &+t\int_{0}^{t}[m^{\infty}(\tau)]d\tau-\frac{t^{3}}{6}\left[e^{2}\right]H(t)-t\left[m^{0}\right]H(t)=0,\end{aligned} \tag{3.7}$$

where

$$[m^{\infty}(t)]=\left([U]^{-1}\right)^{T}[M^{\infty}(t)][U]^{-1}. \tag{3.8}$$

And the coefficient matrices are

$$\begin{aligned}\left[e^1\right] &= \left([U]^{-1}\right)^T\left[E^1\right][U]^{-1} - \frac{s+1}{2}[I],\\ \left[e^2\right] &= \left([U]^{-1}\right)^T\left(\left[E^2\right] - \left[E^1\right]\left[E^0\right]^{-1}\left[E^1\right]^T\right)[U]^{-1},\\ \left[m^0\right] &= \left([U]^{-1}\right)^T\left[M^0\right][U]^{-1}.\end{aligned} \tag{3.9}$$

Once obtained $[m^\infty(t)]$ from (3.7), the acceleration unit-impulse response matrix is obtained as

$$[M^\infty(t)] = [U]^T[m^\infty(t)][U]. \tag{3.10}$$

In this paper, $[M^\infty(t)]$ is obtained using the program SIMILAR presented by Jeremić et al. [48].

4. Calculating Dynamic Load

The dynamic load on the right hand side of (2.7) could be written as follows:

$$\begin{aligned}\{F_r(t)\} &= \{F_r^s(t)\} + \begin{Bmatrix}\{0\}\\ \{F_r^b(t)\}\end{Bmatrix},\\ \{F_r^s(t)\} &= \begin{Bmatrix}\{F_r^{ss}(t)\}\\ \{F_r^{sb}(t)\}\end{Bmatrix},\end{aligned} \tag{4.1}$$

where $\{F_r^s(t)\}$ represents the dynamic load due to ground motion, respectively, and affects the total nodes of the system, while $\{F_r^b(t)\}$ is the dynamic load related to interaction effects and affects the nodes on the foundation-structure interface denoted by b in Figure 2. The dynamic load vector on the right hand side of (2.7) could be written as follows:

$$\begin{Bmatrix}-[M_{ss}]\{\ddot{u}_g\}\\ -[M_{sb}]\{\ddot{u}_g\} - \int_0^t [M^\infty(t-\tau)](\{\ddot{u}_b\})d\tau\end{Bmatrix} = \begin{Bmatrix}-[M_{ss}]\{\ddot{u}_g\}\\ -[M_{sb}]\{\ddot{u}_g\}\end{Bmatrix} + \begin{Bmatrix}\{0\}\\ -\int_0^t [M^\infty(t-\tau)](\{\ddot{u}_b\})d\tau\end{Bmatrix}. \tag{4.2}$$

Comparing (4.1) and (4.2) results

$$\{F_r^s(t)\} = \{-[M]\{\ddot{u}_g\}\}, \tag{4.3}$$

$$\left\{F_r^b(t)\right\} = \left\{-\int_0^t [M^\infty(t-\tau)](\{\ddot{u}_b\})d\tau\right\}, \tag{4.4}$$

where $[M]$ is the total mass matrix of structure, and $[M^{\infty}(t)]$ is the acceleration unit-impulse response matrix.

The dynamic load $F_r^b(t)$ could be written in discrete form as follows [51]:

$$F_r^b(t_n) = \sum_{j=1}^{n} M_{n-j}^{\infty} \int_{(j-1)\Delta t}^{j\Delta t} \ddot{u}_b(\tau)d\tau = \sum_{j=1}^{n} M_{n-j}^{\infty} \left(\dot{u}_{b(j)} - \dot{u}_{b(j-1)}\right), \tag{4.5}$$

where $F_r(t_n)$ is the dynamic load at nth step. $\ddot{u}$ and $\dot{u}$ are the acceleration and velocity at the corresponding time step. In this paper, an iterative method is adopted to calculate $F_r^b(t_n)$. It is supposed that the acceleration is constant at each time step, so (4.5) could be written as follows:

$$F_r^b(t_n) = \sum_{j=1}^{n} M_{n-j}^{\infty} \left(\ddot{u}_{b(j)}\Delta t\right). \tag{4.6}$$

For the first time step, the dynamic load is calculated assuming that $\ddot{u}_b = 0$ (2.7) is solved applying Newmark scheme, and acceleration, velocity, and displacement vectors are obtained. The dynamic load is then calculated using calculated acceleration. Equation (2.7) is solved again and the magnitudes of acceleration, velocity, and displacements are obtained. This procedure is iterated until the convergence is achieved. In this study, the tolerance between two successive iterations is taken as 0.001.

The above procedure is outlined as in Table 1.

According to the above algorithm, an FORTRAN program is prepared to examine the dynamic behavior of the structure considering interaction effects. Numerical examples are presented in the next section.

5. Examples

2D frames on soft ground have been analyzed applying a coupled scaled boundary finite element-Finite element models. The analysis is performed in time domain and the material behavior of soil and structure is assumed to be linear. The soil-structure system is subjected to sine excitations, El Centro, and Tabas ground motions. The displacement and base shear are calculated. Base shear is assumed to be the algebraic summation of horizontal forces induced in the structure. Results are compared with those obtained by cone model.

Example 5.1. As the first example, the frames shown in Figures 2 and 3 are used in analysis. The damping ratio of the structure is considered as five percent of the mass matrix.

Structure properties are assumed as:

$$\begin{aligned} &\text{Frame no. 1:} \quad a = b = 6\,\text{m}, \quad h = 3\,\text{m}, \\ &\text{Frame no. 2:} \quad a = 6\,\text{m}, \quad \text{h} = 3\,\text{m}. \end{aligned} \tag{5.1}$$

The soil properties are

$$\rho = 1600\,\text{kg/m}^3, \quad V_s = 150\,\text{m/s}, \quad \upsilon = 0.3. \tag{5.2}$$

Table 1: The Newmark algorithm and iteration procedure used in the analysis.

(A) Initial conditions	
(1) Form stiffness, mass, and damping matrices of the structure	K, M, C
(2) Initial values	$u^0, \dot{u}^0, \ddot{u}^0$
(3) Select time step and parameters $\alpha = 0.25$, $\delta = 0.5$. Calculate integration constants	$a_0 = \frac{1}{\alpha \Delta t^2}, \quad a_1 = \frac{\delta}{\alpha \Delta t}, \quad a_2 = \frac{1}{\alpha \Delta t}, \quad a_3 = \frac{1}{2\alpha} - 1$ $a_4 = \frac{\delta}{\alpha} - 1, \quad a_5 = \frac{\Delta t}{2}\left(\frac{\delta}{\alpha} - 2\right), \quad a_6 = \Delta t(1-\delta), \quad a_7 = \delta \Delta t$
(4) Form effective stiffness matrix $\widehat{K}$	$\widehat{K} = K + a_0 M + a_1 C$
(B) For each time step	
(1) Use ${}^{t+\Delta t}\ddot{u}_g$ and calculate dynamic load due to ground motion (4.2)	${}^{t+\Delta t}F_r^s$
(2) Iterative procedure	
(2.1) Consider ${}^{t+\Delta t}\ddot{u}_b^k,\ k = 1, 2, 3, \ldots$	${}^{t+\Delta t}\ddot{u}_b^1 = {}^{t}\ddot{u}_b$
(2.2) Calculate the interaction load induced on soil structure interface (4.6) using ${}^{t+\Delta t}\ddot{u}_b^k$	${}^{t+\Delta t}F_r^b$
(2.3) Calculate the dynamic load ${}^{t+\Delta t}R$	${}^{t+\Delta t}R = \begin{Bmatrix} {}^{t+\Delta t}F_r^{ss} \\ {}^{t+\Delta t}F_r^{sb} + {}^{t+\Delta t}F_r^{b} \end{Bmatrix}$
(2.4) Calculate effective load $\widehat{R}$ at time $t + \Delta t$	${}^{t+\Delta t}\widehat{R} = {}^{t+\Delta t}R + M(a_0\,{}^{t}U + a_2\,{}^{t}\dot{U} + a_3\,{}^{t}\ddot{U}) + C(a_1\,{}^{t}U + a_4\,{}^{t}\dot{U} + a_5\,{}^{t}\ddot{U})$
(2.5) Applying Gauss reduction scheme, displacements are calculated at time $t + \Delta t$	$\widehat{K}\,{}^{t+\Delta t}U = {}^{t+\Delta t}\widehat{R}$
(2.6) Calculate acceleration and velocities at time $t + \Delta t$	${}^{t+\Delta t}\ddot{U}^{k+1} = \begin{Bmatrix} \ddot{u}_s^{k+1} \\ \ddot{u}_b^{K+1} \end{Bmatrix} = a_0({}^{t+\Delta t}U - {}^{t}U) - a_2\,{}^{t}\dot{U} - a_3\,{}^{t}\ddot{U}$ ${}^{t+\Delta t}\dot{U} = {}^{t}\dot{U} + a_6\,{}^{t}\ddot{U} + a_7\,{}^{t+4\Delta t}\ddot{U}$
(2.7) Calculate the tolerance between two successive iterations	$\mathrm{TLR} = \left\| {}^{t+\Delta t}\ddot{u}_b^{K+1} - {}^{t+\Delta t}\ddot{u}_b^{K} \right\|$
(2.8) Check TLR. If TLR < 0.001, the iterative procedure finishes otherwise steps 2.2 to 2.8 are repeated using ${}^{t+\Delta t}\ddot{u}_b^{k+1}$	

Table 2: Properties of structural elements.

Element	r (kgf/m^3)	A (m^2)	I (m^4)	E (kgf/m^2)
Beam	2400	0.36	$1.08E-2$	$2.531E9$
Column	2400	0.36	$1.08E-2$	$2.531E9$

Firstly, a dynamic analysis is performed (ignoring SSI effects). The natural frequencies and periods of the structures are calculated and presented in Tables 3 and 4. Then the soil-structure system is subjected to sine excitations with unit amplitude. The loading frequency is con-

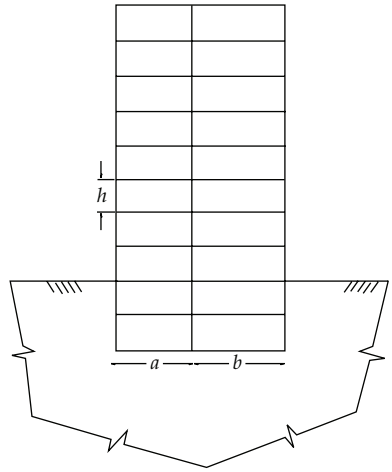

Figure 2: Frame no. 1 used in analysis.

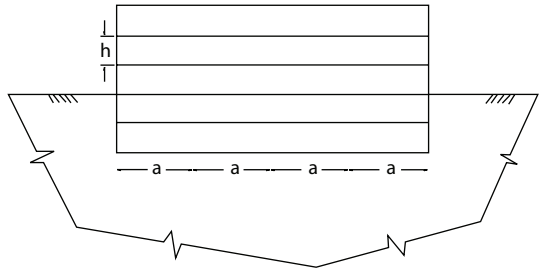

Figure 3: Frame no. 2 used in analysis.

Table 3: Natural frequencies and periods of first five modes of frame no. 1.

Modes	Natural frequency (Hz)	Period (s)
First mode	0.84	1.189
Second mode	2.579	0.388
Third mode	4.474	0.224
Fourth mode	6.594	0.152
Fifth mode	8.959	0.112

Table 4: Natural frequencies and periods of first five modes of frame no. 2.

Modes	Natural frequency (Hz)	Period (s)
First mode	1.66	0.603
Second mode	5.24	0.191
Third mode	9.41	0.106
Fourth mode	13.93	0.072
Fifth mode	17.64	0.057

Table 5: Relative reduction of displacement and base shear considering SSI effects for frame no. 1 subjected to sine excitation.

Maximum of	Relative reduction (%)	
	First mode	Second mode
Displacement	15.3	35.6
Base shear	12.7	60.65

Table 6: Relative reduction of displacement and base shear considering SSI effects for frame no. 2 subjected to sine excitation.

Maximum of	Relative reduction (%)	
	First mode	Second mode
Displacement	40.9	41.3
Base shear	63.8	82

Table 7: Relative reduction of displacement and base shear considering SSI effects for frame no. 1 subjected to El Centro ground motion.

Maximum of	Displacement (cm)	Base shear (Kgf)
Dynamic analysis ignoring SSI effect	10.9	214855
Dynamic analysis considering SSI effect	7.55	109885
Relative reduction (%)	30.73	48.75

Table 8: Relative reduction of displacement and base shear considering SSI effects for frame no. 2 subjected to El Centro ground motion.

Maximum of	Displacement (cm)	Base shear (Kgf)
Dynamic analysis ignoring SSI effect	6.61	357693
Dynamic analysis considering SSI effect	2.63	149835
Relative reduction (%)	60.2	58.1

sidered to be variable and selected so that it would be close to natural frequencies of the structure. The harmonic load used in the analysis could be expressed as follows:

$$F = \sin\left(\frac{2\pi}{T}t\right), \tag{5.3}$$

where T is the period of sine function. The SSI effect on dynamic response of the structure is examined. Figures 4, 5, 6, 7, 8, 9, 10, 11, 12, 13, 14, 15, and 16 show the results obtained in analysis. Figures 17, 18, 19, and 20 show the variation of displacement and base shear versus period of dynamic load. The maximums (peaks) represent the obtained magnitudes with loading period close to the first and the second natural periods of the structure. As can be seen considering SSI effects, the maximum displacement and base shear are decreased. In Tables 5 and 6 the percentage of the relative reduction of displacement and base shear due to first and second modes is presented.

It is observed that considering SSI effect leads to reduction in displacement and base shear. The reduction in displacement and base shear is more significant when the loading frequency is close to natural frequencies of the structure. As shown in Tables 5 and 6, the

Table 9: Relative reduction of displacement and base shear considering SSI effects for frame no. 1 subjected to Tabas ground motion.

Maximum of	Displacement (cm)	Base shear (Kgf)
Dynamic analysis ignoring SSI effect	8.58	194230
Dynamic analysis considering SSI effect	4.03	41399
Relative reduction (%)	53	78.6

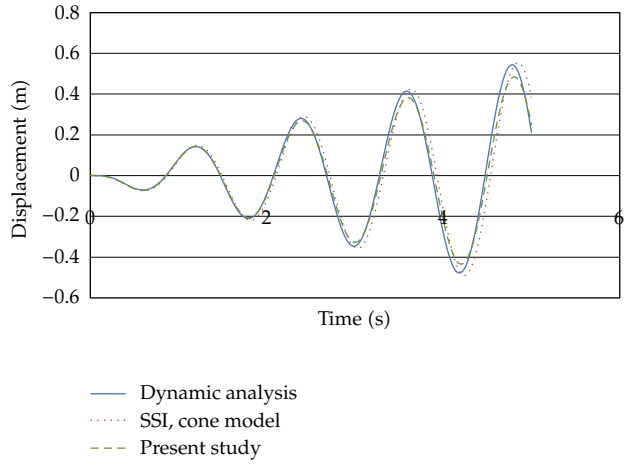

Figure 4: Comparison of displacement at the top of frame no. 1 subjected to sine excitation ($T = 1.2$ s).

Table 10: Relative reduction of displacement and base shear considering SSI effects for frame no. 2 subjected to Tabas ground motion.

Maximum of	Displacement (cm)	Base shear (Kgf)
Dynamic analysis ignoring SSI effect	5.86	367403
Dynamic analysis considering SSI effect	2.19	102447
Relative reduction (%)	62.6	72.1

percentage of relative reduction in displacement and base shear is more significant for the second mode than the first one. It could be concluded that SSI effect is more pronounced for higher modes of the structure. Comparing the results presented in Tables 5 and 6 shows that the relative reduction is more significant for farme no. 2. It could be concluded that SSI effects are more significant for stiff structures.

Example 5.2. In the second example, the fames are subjected to El Centro ground motion. It is worth noting that the predominant period of El Centro ground motion is 0.56 (sec) which is close to the first natural period of frame no. 2. The results are given in Figures 21, 22, 23, and 24. As can be observed in Tables 7 and 8, the relative reduction in displacement and shear base is more significant for frame no. 2. It can be concluded that when the predominant period of the earthquake is close to natural period of the structure, considering SSI effects leads to more significant reduction, and the dynamic response of the structure is more affected.

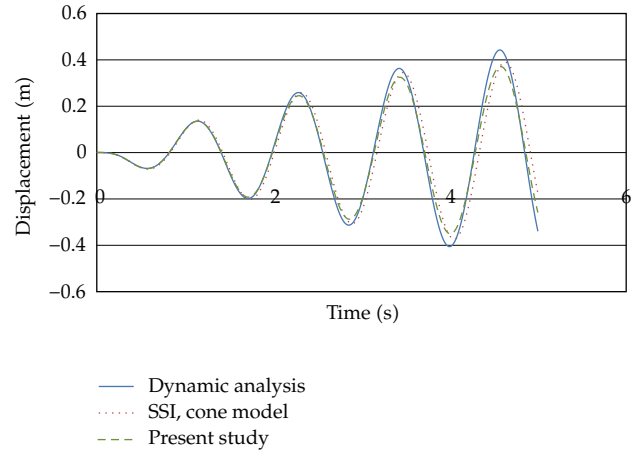

Figure 5: Comparison of displacement at the top of frame no. 1 subjected to sine excitation (T = 1.1 s).

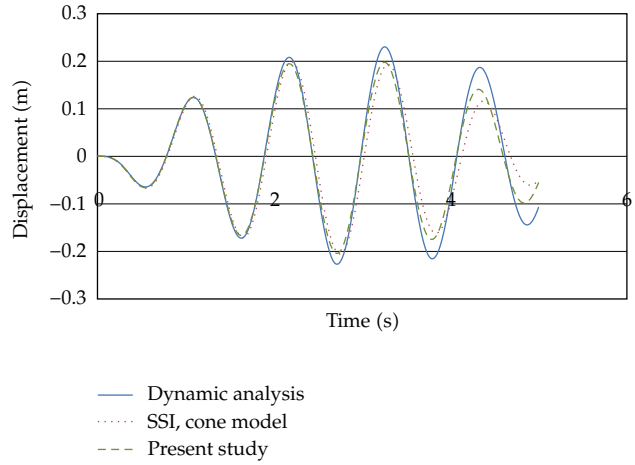

Figure 6: Comparison of displacement at the top of frame no. 1 subjected to sine excitation (T = 1 s).

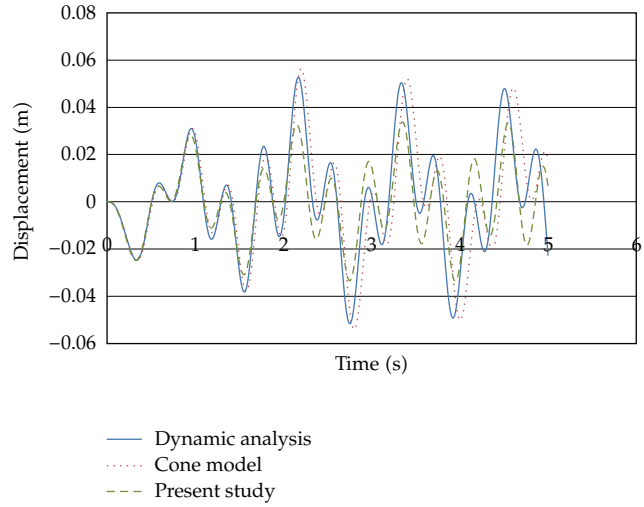

Figure 7: Comparison of displacement at the top of frame no. 1 subjected to sine excitation (T = 0.4 s).

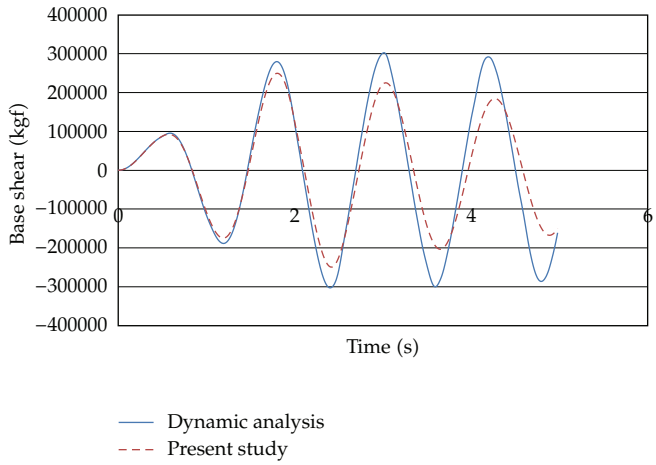

Figure 8: Comparison of base shear of frame on. 1 subjected to sine excitation ($T = 1.2$ s).

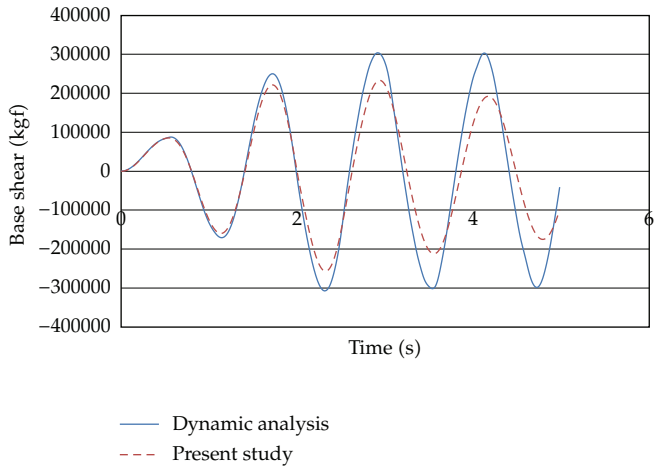

Figure 9: Comparison of base shear of frame no. 1 subjected to sine excitation ($T = 1.1$ s).

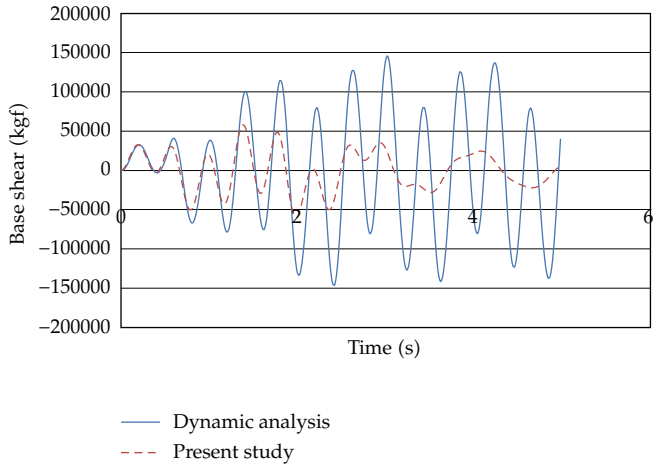

Figure 10: Comparison of base shear of frame no. 1 subjected to sine excitation ($T = 0.4$ s).

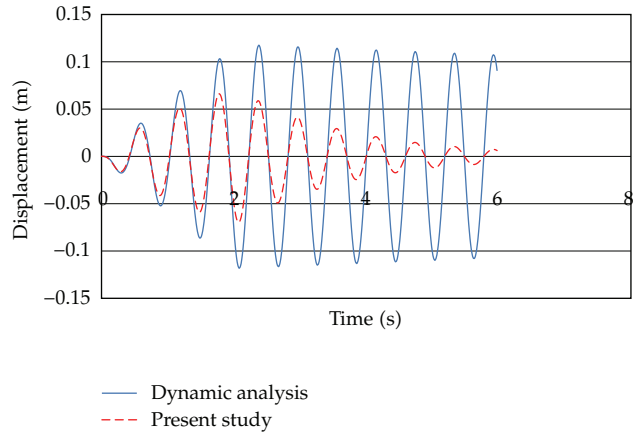

Figure 11: Comparison of displacement at top of frame no. 2 subjected to sine excitation ($T = 0.6$ s).

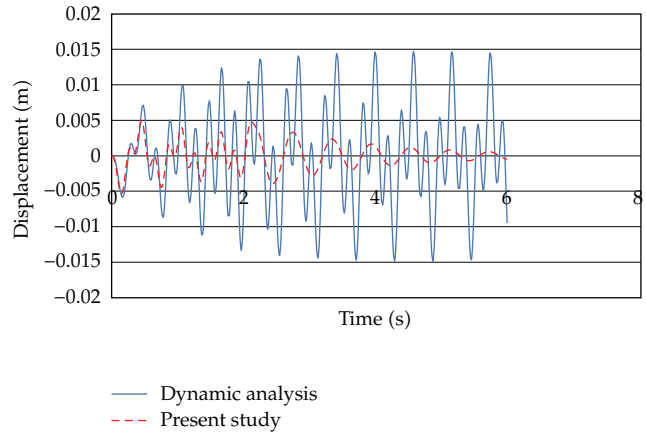

Figure 12: Comparison of displacement at top of frame no. 2 subjected to sine excitation ($T = 0.2$ s).

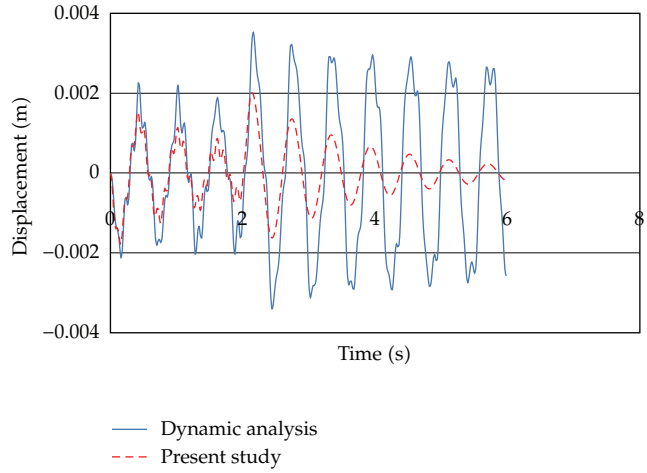

Figure 13: Comparison of displacement at top of frame no. 2 subjected to sine excitation ($T = 0.1$ s).

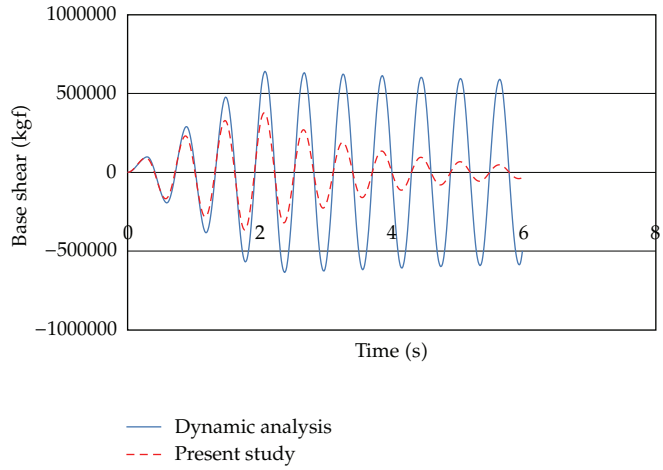

Figure 14: Comparison of base shear of frame no. 2 subjected to sine excitation ($T = 0.6$ s).

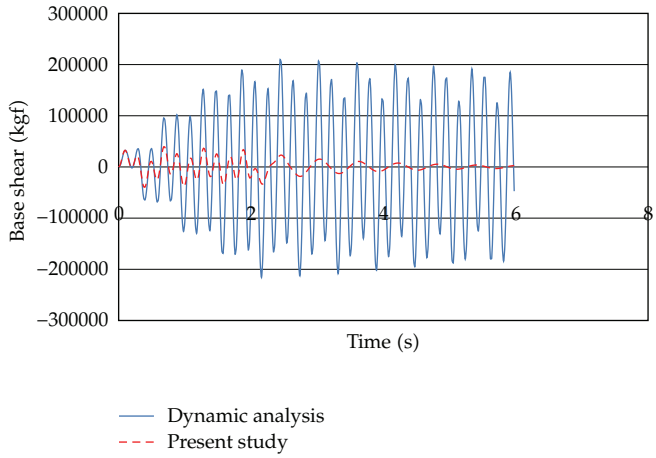

Figure 15: Comparison of base shear of frame no. 2 subjected to sine excitation ($T = 0.2$ s).

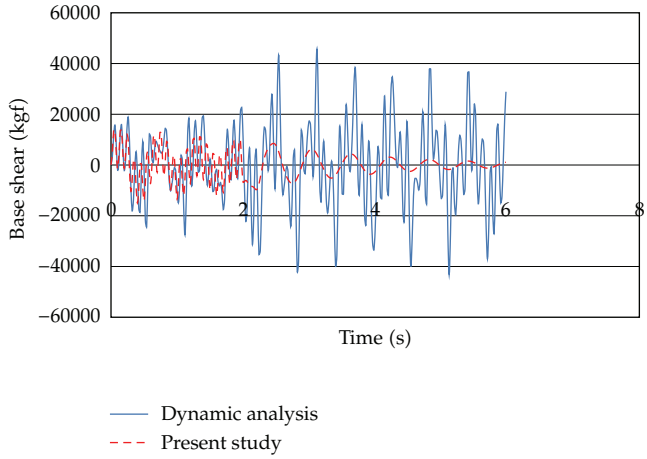

Figure 16: Comparison of base shear of frame no. 2 subjected to sine excitation ($T = 0.1$ s).

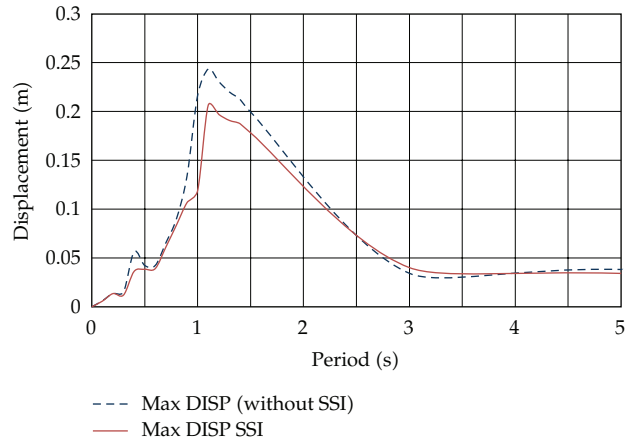

Figure 17: Comparison of displacement at top of frame no. 1.

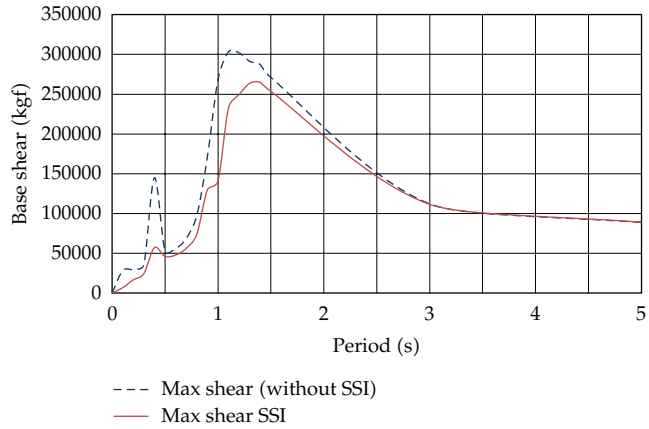

Figure 18: Comparison of base shear of frame no. 1.

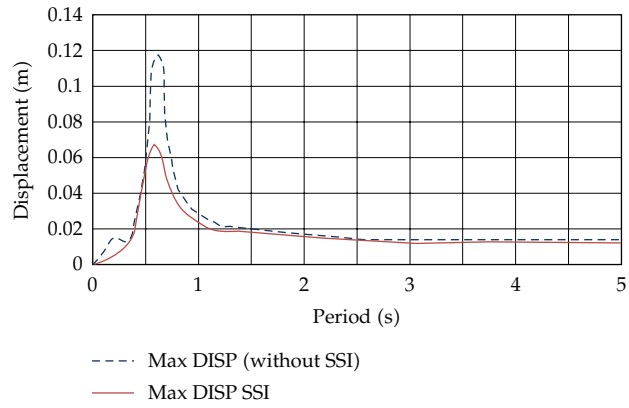

Figure 19: Comparison of displacement at top of frame no. 2.

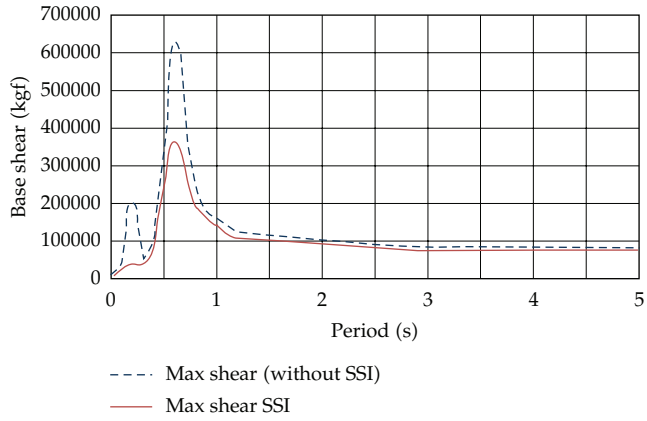

Figure 20: Comparison of base shear of frame no. 2.

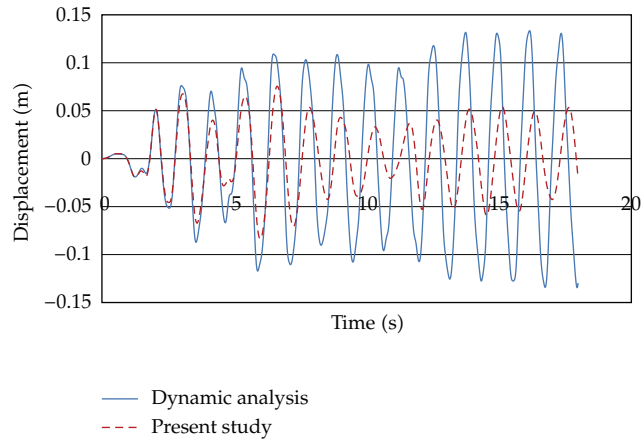

Figure 21: Comparison of displacement at the top of frame no. 1 subjectefd to El Centro ground motion.

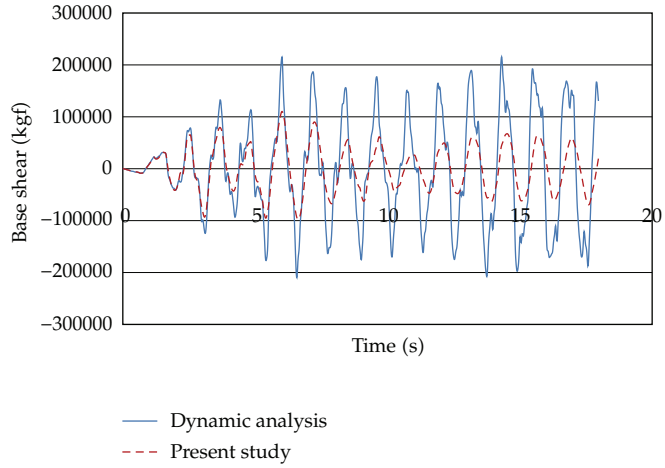

Figure 22: Comparison of base shear of frame no. 1 subjected to El Centro ground motion.

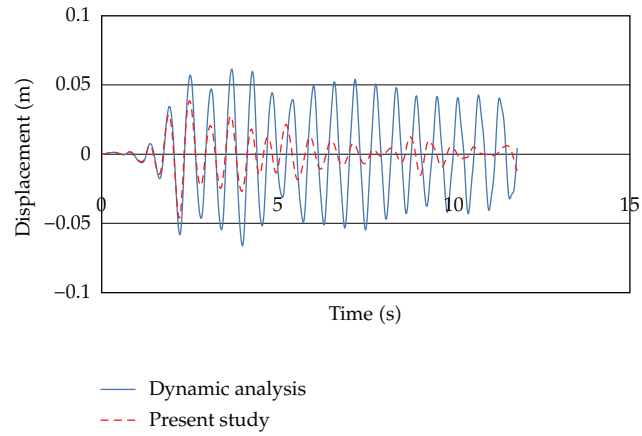

Figure 23: Comparison of displacement at the top of frame no. 2 subjected to El Centro ground motion.

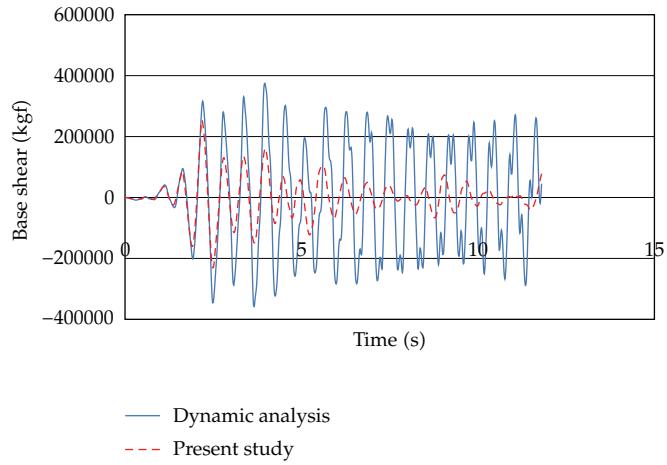

Figure 24: Comparison of base shear of frame no. 2 subjected to El Centro ground motion.

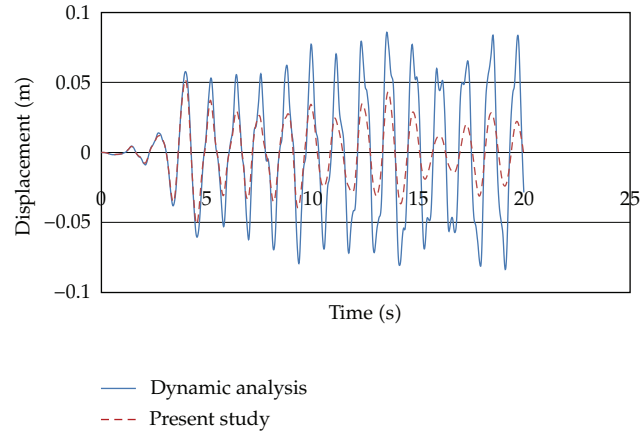

Figure 25: Comparison of displacement at top of frame no. 1 subjected to Tabas ground motion.

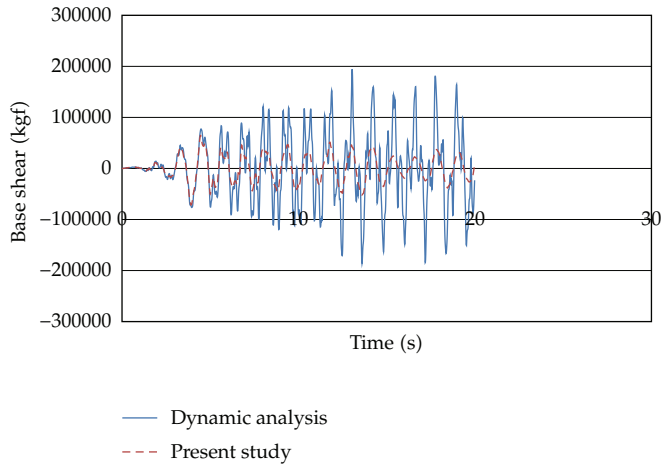

Figure 26: Comparison of base shear of frame no. 1 subjected to Tabas ground motion

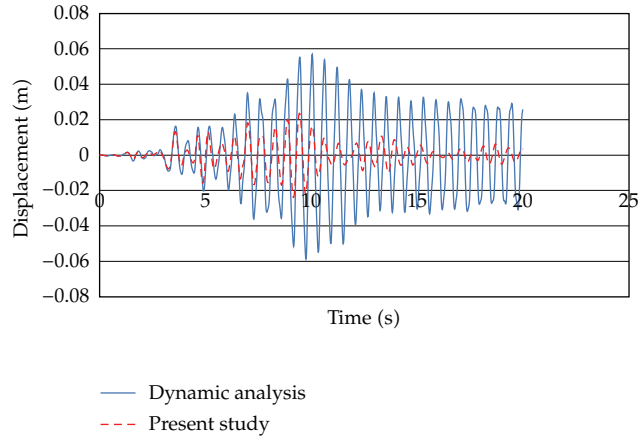

Figure 27: Comparison of displacement at the top of frame no. 2 subjected to Tabas ground motion.

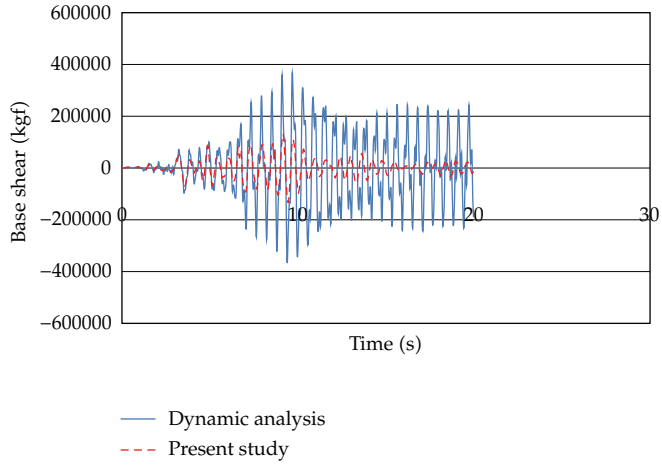

Figure 28: Comparison of base shear of frame no. 2 subjected to Tabas ground motion.

Example 5.3. In the third example, the frames are subjected to Tabas ground motion. The predominant period of Tabas ground motion is 0.2 (sec) which is close to the second natural period of frame no. 2. The results are given in Figures 25, 26, 27, and 28. As it is observed, considering SSI effect has a pronounced effect on results (Tables 9 and 10).

6. Conclusion

Analysis and design of structures subjected to arbitrary dynamic loadings especially earthquakes have been studied during past decades. In practice, the effects of soil-structure interaction on the dynamic response of structures are usually neglected. In this paper, a coupled scaled boundary finite element-finite element model is presented to examine the dynamic response of the structure considering soil-structure interaction. The substructure method is used to analyze the soil-structure interaction problem. The analysis is performed in time domain. The material behavior of soil and structure is assumed to be linear. The scaled boundary finite element method is used to calculate the dynamic stiffness of the soil, and the finite element method is applied to analyze the dynamic behavior of the structure. 2D frames have been analyzed using the proposed model. The results are compared with those obtained by cone model. Considering SSI effect leads to reduction in displacement and base shear. When the system is subjected to sine excitation, the reduction in displacement and base shear is more significant when the loading frequency is close to natural frequencies of the structure. The reduction in displacement and base shear is more significant for the second mode than the first one, thus considering SSI in dynamic analysis of the structure affects the higher modes more significantly. It is observed that when the soil-structure system is subjected to an earthquake whose predominant period is close to natural period of the structure, considering SSI effects leads to more significant reduction, and the dynamic response of the structure is more affected. It is obvious that considering SSI effects results in more effective design without decreasing safety margin.

References

[1] J. E. Luco, "Soil-structure interaction and identification of structural models," in *Proceedings of the ASCE Specialty Conference in Civil Engineering and Nuclear Power*, Tenn, USA, 1980.
[2] J. P. Wolf, *Dynamic Soil-Structure Interaction*, Prentice Hall, Englewood Cliffs, NJ, USA, 1985.
[3] J. Avilés and L. E. Pérez-Rocha, "Evaluation of interaction effects on the system period and the system damping due to foundation embedment and layer depth," *Soil Dynamics and Earthquake Engineering*, vol. 15, no. 1, pp. 11–27, 1996.
[4] R. W. Clough and J. Penzien, *Dynamics of Structures*, McGraw-Hill, New York, NY, USA, 2003.
[5] P. C. Jennings and J. Bielak, "Dynamics of building-soil interaction," *Bulletin of the Seismological Society of America*, vol. 63, pp. 9–48, 1973.
[6] A. S. Veletsos and V. V. D. Nair, "Seismic interaction of structures on hysteretic foundations," *Journal of the Structural Division*, vol. 101, no. 1, pp. 109–129, 1975.
[7] J. Bielak, "Dynamic behavior of structures with embedded foundations," *Earthquake Engineering and Structural Dynamics*, vol. 3, no. 3, pp. 259–274, 1975.
[8] M. I. Todorovska and M. D. Trifunac, "The system damping, the system frequency and the system response peak amplitudes during in-plane building-soil interaction," *Earthquake Engineering and Structural Dynamics*, vol. 21, no. 2, pp. 127–144, 1992.
[9] J. Aviles and L. E. Perez-Rocha, "Effects of foundation embedment during building-soil interaction," *Earthquake Engineering and Structural Dynamics*, vol. 27, no. 12, pp. 1523–1540, 1998.
[10] R. Betti, A. M. Abdel-Ghaffar, and A. S. Niazy, "Kinematic soil-structure interaction for long-span cable-supported bridges," *Earthquake Engineering and Structural Dynamics*, vol. 22, no. 5, pp. 415–430, 1993.

[11] J. Aviles, M. Suarez, and F. J. Sanchez-Sesma, "Effects of wave passage on the relevant dynamic properties of structures with flexible foundation," *Earthquake Engineering and Structural Dynamics*, vol. 31, pp. 139–159, 2002.
[12] J. P. Wolf, *Foundation Vibration Analysis Using Simple Physical Models*, Prentice Hall, Englewood Cliffs, NJ, USA, 1994.
[13] J. Lysmer and R. L. Kuhlemeyer, "Finite dynamic model for infinite media," *Journal of Engineering Mechanics Division*, vol. 95, no. 4, pp. 859–877, 1969.
[14] W. D. Smith, "A nonreflecting plane boundary for wave propagation problems," *Journal of Computational Physics*, vol. 15, no. 4, pp. 492–503, 1974.
[15] R. Clayton and B. Engquist, "Absorbing boundary conditions for acoustic and elastic wave equations," *Bulletin of the Seismological Society of America*, vol. 67, pp. 1529–1540, 1977.
[16] W. White, S. Valliappan, and I. K. Lee, "Unified boundary for finite dynamic models," *Journal of Engineering Mechanics*, vol. 103, no. 5, pp. 949–964, 1977.
[17] Z. P. Liao and H. L. Wong, "A transmitting boundary for the numerical simulation of elastic wave propagation," *International Journal of Soil Dynamics and Earthquake Engineering*, vol. 3, no. 4, pp. 174–183, 1984.
[18] F. Medina and R. L. Taylor, "Finite element techniques for problems of unbounded domains," *International Journal for Numerical Methods in Engineering*, vol. 19, no. 8, pp. 1209–1226, 1983.
[19] G. D. Manolis and D. E. Beskos, *Boundary Element Methods in Elastodynamics*, Unwin Hyman, London, UK, 1988.
[20] J. Dominguez, *Boundary Elements in Dynamics*, Computational Mechanics Publications, Southampton, UK, 1993.
[21] D. E. Beskos, "Boundary element methods in dynamic analysis: part II (1986–1996)," *Applied Mechanics Reviews*, vol. 50, no. 3, pp. 149–197, 1997.
[22] W. S. Hall and G. Oliveto, *Boundary Element Methods for Soil-Structure Interaction*, Kluwer Academic, Dodrecht, The Netherlands, 2003.
[23] J. W. Meek and J. P. Wolf, "Cone models for homogeneous soil. I," *Journal of the Geotechnical Engineering Division*, vol. 118, no. 5, pp. 667–685, 1992.
[24] J. W. Meek and J. P. Wolf, "Cone models for soil layer on rigid rock. II," *Journal of the Geotechnical Engineering Division*, vol. 118, no. 5, pp. 686–703, 1992.
[25] J. W. Meek and J. P. Wolf, "Cone models for nearly incompressible soil," *Earthquake Engineering and Structural Dynamics*, vol. 22, no. 8, pp. 649–663, 1993.
[26] J. W. Meek and J. P. Wolf, "Cone models can present the elastic half-space," *Earthquake Engineering and Structural Dynamics*, vol. 22, no. 9, pp. 759–771, 1993.
[27] J. W. Meek and J. P. Wolf, "Cone models for embedded foundation II," *Journal of the Geotechnical Engineering Division*, vol. 120, no. 1, pp. 60–80, 1994.
[28] J. P. Wolf and J. W. Meek, "Cone models for a soil layer on a flexible rock half-space," *Earthquake Engineering and Structural Dynamics*, vol. 22, no. 3, pp. 185–193, 1993.
[29] J. P. Wolf and J. W. Meek, "Rotational cone models for a soil layer on flexible rock half-space," *Earthquake Engineering and Structural Dynamics*, vol. 23, no. 8, pp. 909–925, 1994.
[30] J. P. Wolf and J. W. Meek, "Dynamic stiffness of foundation on layered soil half-space using cone frustums," *Earthquake Engineering and Structural Dynamics*, vol. 23, no. 10, pp. 1079–1095, 1994.
[31] R. F. Ungless, *An infinite element*, M.S. thesis, University of British Columbia, 1973.
[32] P. Bettess, "Infinite elements," *International Journal for Numerical Methods in Engineering*, vol. 11, no. 1, pp. 53–64, 1977.
[33] P. Bettes, *Infinite Elements*, Penshaw Press, Sunderland, UK, 1992.
[34] J. P. Wolf and C. Song, *Finite Element Modeling of Unbounded Media*, Wiley, UK, 1996.
[35] J. P. Wolf, *The Scaled Boundary Finite Element Method*, Wiley, UK, 2003.
[36] D. L. Karabalis and D. E. Beskos, "Dynamic response of 3-D flexible foundations by time domain BEM and FEM," *International Journal of Soil Dynamics and Earthquake Engineering*, vol. 4, no. 2, pp. 91–101, 1985.
[37] O. V. Estorff, "Dynamic response of elastic blocks by time domain BEM and FEM," *Computers and Structures*, vol. 38, no. 3, pp. 289–300, 1991.
[38] F. Guan and M. Novak, "Transient response of an elastic homogeneous half-space to suddenly applied rectangular loading," *Transactions of the ASME*, vol. 61, no. 2, pp. 256–263, 1994.
[39] J. Qian, L. G. Tham, and Y. K. Cheung, "Dynamic cross-interaction between flexible surface footings by combined BEM and FEM," *Earthquake Engineering and Structural Dynamics*, vol. 25, no. 5, pp. 509–526, 1996.

[40] O. Von Estorff and M. J. Prabucki, "Dynamic response in the time domain by coupled boundary and finite elements," *Computational Mechanics*, vol. 6, no. 1, pp. 35–46, 1990.

[41] A. S. M. Israil and P. K. Banerjee, "Effects of geometrical and material properties on the vertical vibration of three-dimensional foundations by BEM," *International Journal for Numerical and Analytical Methods in Geomechanics*, vol. 14, no. 1, pp. 49–70, 1990.

[42] X. Zhang, J. L. Wegner, and J. B. Haddow, "Three-dimensional dynamic soil-structure interaction analysis in the time domain," *Earthquake Engineering and Structural Dynamics*, vol. 28, no. 12, pp. 1501–1524, 1999.

[43] A. H. Tanrikulu, H. R. Yerli, and A. K. Tanrikulu, "Application of the multi-region boundary element method to dynamic soil-structure interaction analysis," *Computers and Geotechnics*, vol. 28, no. 4, pp. 289–307, 2001.

[44] C. B. Yun, D. K. Kim, and J. M. Kim, "Analytical frequency-dependent infinite elements for soil-structure interaction analysis in two-dimensional medium," *Engineering Structures*, vol. 22, no. 3, pp. 258–271, 2000.

[45] D. K. Kim and C. B. Yun, "Time domain soil-structure interaction analysis in two dimensional medium based on analytical frequency-dependent infinite elements," *International Journal for Numerical Methods in Engineering*, vol. 47, no. 7, pp. 1241–1261, 2000.

[46] D. K. Kim and C. B. Yun, "Earthquake response analysis in the time domain for 2D soil-structure systems using analytical frequency-dependent infinite elements," *International Journal for Numerical Methods in Engineering*, vol. 58, no. 12, pp. 1837–1855, 2003.

[47] M. C. Genes and S. Kocak, "Dynamic soil-structure interaction analysis of layered unbounded media via a coupled finite element/boundary element/scaled boundary finite element model," *International Journal for Numerical Methods in Engineering*, vol. 62, no. 6, pp. 798–823, 2005.

[48] B. Jeremić, G. Jie, M. Preisig, and N. Tafazzoli, "Time domain simulation of soil-foundation-structure interaction in non-uniform soils," *Earthquake Engineering and Structural Dynamics*, vol. 38, no. 5, pp. 699–718, 2009.

[49] M. Mahsuli and M. A. Ghannad, "The effect of foundation embedment on inelastic response of structures," *Earthquake Engineering and Structural Dynamics*, vol. 38, no. 4, pp. 423–437, 2009.

[50] J. P. Wolf and Ch. Song, *Finite-Element Modelling of Unbounded Media*, John Wiley & Sons, Chichester, UK, 1996.

[51] L. Lehmann, *Wave Propagation in Infinite Domains with Applications to Structure Interaction*, Springer, Berlin, Germany, 2007.